RPC-TN-18
August 10, 2001

Spectrometer for E160

P. Bosted, P. Decowski, and K. Griffioen

Abstract

The layout of a spectrometer for E160 based on the E158 D3 dipole is presented, along with the design of the beam pipe, shielding, and hadron filter. An outline of the detector arrangement is also given. Background rates from hadronic punch-through, atomic Compton scattering, Primakov π^0 production, and muon and electron pair production in the target are listed. The acceptance of the spectrometer for J/ψ events is shown, as are resolutions and counting rates.

1 Introduction

The spectrometer and detector design presented in this report is based on a detailed study of the physics requirements [1] and a general study of several spectrometer design options that could meet these requirements [2]. This study concluded that a spectrometer based on the existing D3 magnet (this is the E158 name) would be the most effective, and the present report gives details of all the important aspects of this design.

2 Physical Layout

2.1 Magnet

The D3 dipole magnet will remain in the same physical location as E158, which means the magnet is centered on the E.S.A. beam axis vertically, and parallel to it horizontally, but centered 7 cm to the north. A study using bosted/jpsi/d3spect.f showed that there is no significant change in the acceptance with a 7 cm offset, in any of the important parameters such as the transverse momentum of the J/ψ particles. There is a small shift in the $\cos(\theta_{cm})$ distribution, which can be averaged out by occasionally reversing the polarity of D3. Fig. 1 shows plan and elevation views of the D3 magnet, along with outlines of the target, hadron filter, beam pipe, collimator, and detectors.

The overall dimensions of the D3 magnet iron are 345 cm long, ± 87 cm tall, and ± 116.2 cm wide. The coils are of the "elephant ear" design, and extend about 35 cm on the west (up-beam) side and 30 cm on the east (down-beam) end of the magnet.

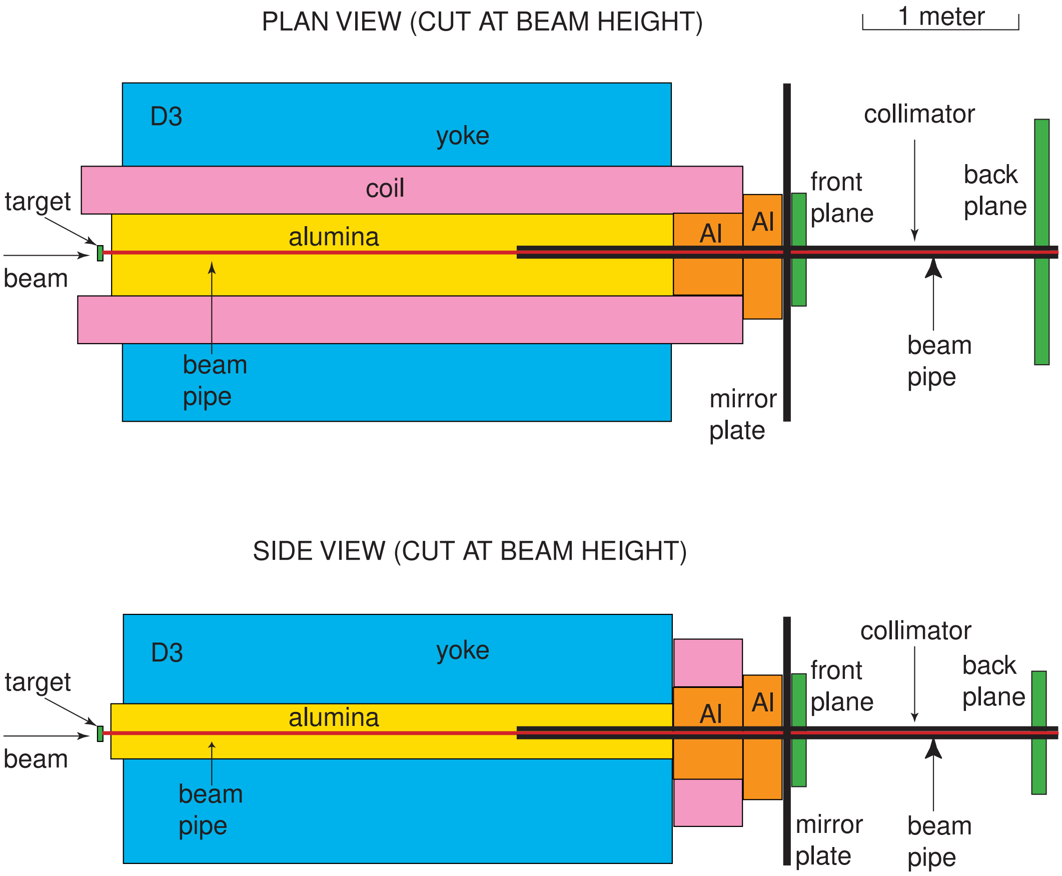

Figure 1: Principal elements of the E160 spectrometer in ESA. The beam pipe and collimator are drawn wider than true scale for clarity.

2.2 Utilities for D3

For E158, D3 runs at 1100 amps, while for E160 we will run close to 2700 amps in order to obtain as high a magnetic field as possible (above 22 kG). This will require the use of one of the two 1.59 MW power supplies in building 208. The magnet is presently connected to one of these (B203). Presently there are only three 500 A cables going from the pivot area to the magnet on the supply and return legs: to run at 2700 amps, three additional 500 A cables will need to be installed on each leg. At 2700 A, D3 will draw close to 1.5 MW of power, requiring a water flow of about 150 gpm. Presently, the water flow is about 40 gpm. Lager hoses will be needed to allow the higher flow rate from the master supply pipe. The flow in D2 can be reduced if necessary to allow enough pressure.

3 Target

The design location for the solid target assembly is 15 cm up-beam of the yoke of D3. For more details, see [3].

Table 1: Dimensions of the collimator that fits around the beam pipe. The beam direction is z, with $z = 0$ the target location, and y is vertical. For tungsten, a "heavy met" alloy is assumed with a density of about 18 gm/cm^3.

z-range	x	y	material	volume	weight
260-360 cm	±5.0 cm	±2.6 cm	tungsten	4900 cm^3	88 kg
360-420 cm	±5.0 cm	±3.5 cm	tungsten	5100 cm^3	73 kg
420-580 cm	±5.0 cm	±4.4 cm	tungsten	13700 cm^3	250 kg

4 Beam Pipe

Based on the beam optics study in [4], it is necessary to have a beam pipe diameter (in vacuum) of at least 17 mm to avoid the tails of the photon beam directly hitting the vacuum pipe. This value is therefore picked as the inner diameter of the vacuum beam pipe, which should be welded to the target changer chamber. The pipe should be about 6 m long, extending through D3 and the detectors. Beyond this, it can be connected to the E158 vacuum system by another bellows. The pipe thickness should be as thin as reasonably practical, and can be made either of aluminum or stainless steel.

It is crucial that the beam pipe be round to within ±0.25 mm, and that is be aligned with the beam axis to ±0.3 mm over the full length of the pipe.

4.1 Beam Pipe Collimator

Because of the large number of Compton scattered photons that hit the inside of the beam pipe all along its length, the pipe must be surrounded by high-Z material. In the vertical direction, the collimator must stay below the 10 mr minimum angle that we wish to have for J/ψ decay muons. In the horizontal direction, the collimator can be wider, but not so wide as to cause unwanted Bethe-Heitler muon to multiple scatter into the detectors.

Several designs were investigated with the GEANT Monte Carlo (for more details, see bosted/E160/geant/notes.m1). It was found that using tungsten gives about a factor of three lower backgrounds than using lead, so we would like to use tungsten if possible. The collimator can be divided into several sections, with the z range and cross sectional areas listed in Table 1. Each rectangular cross section segment should have a hole cut in the center large enough for the beam pipe to fit through (about 18 mm diameter). The collimator sections can be made of many individual pieces, if desired, but should fit reasonably snugly around the beam pipe, with minimal aligned gaps along the beam direction (for example, the gaps could alternate between vertical and horizontal).

Under investigation is the option of making a square aperture around the beam pipe, rather than a round one. This would likely make construction much simpler, as only rectangular plates of tungsten would be needed.

Table 2: Approximate Dimensions of the filter that fits around the beam pipe and collimators. The beam direction is z, with $z = 0$ the target location, and y is vertical.

z-range	x	y	material	weight
5-360 cm	± 27.4 cm	± 17.4 cm	alumina	2400 kg
360-410 cm	± 27.4 cm	± 30 cm	aluminum	440 kg
410-440 cm	± 40.0 cm	± 40 cm	aluminum	520 kg

4.2 Hadron Filter

As shown in [2], alumina is the optimal choice for the hadron filter. The studies assume that it can be obtained in a density of about 3.6 gm/cm^2 (higher than powder, but lower than the expensive high density ceramics). The filter should begin about 5 cm down-beam of the target, and extend to the end of the iron in D3. This makes for a volume 355 cm long, ± 27.5 cm wide, and ± 17.4 cm tall, so that it fits snugly between the magnet coils and pole faces. It could be made of top and bottom pieces, in order to accommodate a central opening for the beam pipe and collimator, but it is important to minimize any long gaps in the beam direction, either by making the gap very small (< 0.1 mm), or by staggering the gaps vertically by using several longitudinal segments. The total weight of the alumina is about 2,500 kg.

The pole faces of D3 have double flares at each end of the magnet. It is not necessary to fill in the flare at the up-beam end, but the down beam end flares should be filled with alumina if possible, or aluminum if alumina is too difficult.

Beyond D3, we would like to have two segments of aluminum, totaling 80 cm, between end of the D3 yoke, and the beginning of the mirror plate. The first segment covers the z distance of the magnet coils (about 50 cm), and should fit snugly between them. This piece must be rounded on the corners to match the coil geometry. The second segment is wider and taller than the first segment. The approximate dimensions are given in Table 2. Both segments should have a central opening large enough to snugly fit around the collimator pieces. Each segment could be made as a right and left half, and should be mounted in such a way that it is reasonably easy to remove them during the experiment. If background rates are low enough, we may want to remove them to obtain better resolution, at the expense of somewhat higher background rates.

Suitable stands will be needed to hold the aluminum pieces beyond D3. It should be possible to align the pieces so that they fit snugly around the collimator, without stressing the beam pipe. The alumina inside D3 can be supported by the pole face.

4.3 Mirror Plate

An iron mirror plate with a thickness of about 4 cm will be placed 80 cm down-beam of the end of the yoke of D3. The outer dimensions of the plate should match those of the magnet (± 87 cm tall and ± 116.2 cm wide). There should be a hole cut in the center matched to the dimensions of the last segment of the collimator (±5.0 cm wide and ±4.4 cm tall). A stand will be needed to support the mirror plate (the same stand can be used to support the front hodoscope detectors), and tie rods connecting the corners of the mirror plate to the dipole will be needed to avoid the plate being sucked into the magnet, when energized.

5 Detector arrangement

5.1 Introduction

We plan to have three hodoscope planes, one 85 cm from the end of the D3 iron ("front"), one 150 cm further down-beam ("back"), and a final one another 75 cm down-beam ("muon"). An iron wall between the back and muon planes will be used to stop pions and protons, providing a positive muon identification in most cases. Stands will be needed to support these detector frames, and the Q1 quad will have to be removed to make space for them.

The layout of each frame looks like a "bow-tie" or "chevron", with a vertical slope of 0.17 radians away from the "sheet of flame" of Bethe-Heitler muons at the beam height. This is illustrated in Fig. 2, which shows the overall dimensions of the front and back planes, along with the distribution of hits expected from J/ψ particles at 15 and 35 GeV. Note that the 35 GeV decay muons are concentrated close to $x = 0$.

Studies using bosted/jpsi/d3spect.f show that with a spacing of 1.5 m between the front and back hodoscope planes, a granularity of about 4 mm to 5 mm is needed so that the hodoscopes do not have a significant influence on the reconstructed J/ψ mass spectra. Using existing fine grained hodoscopes, there are not quite enough to cover the area needed to maximize the solid angle, so we propose to put these in the region where over 90% of the 25 and 35 GeV J/ψ tracks go. This corresponds to $x = \pm25$ cm in the front plane, and $x = \pm60$ cm in the back plane. The fine resolution region will be covered with fingers from E155 that are either 1.27 cm or 1.5 cm wide.

We assume that new hodoscopes fingers should be about 2.54 cm wide to match the width of the proposed PMT's. These will cover a wider region in x, overlapping the fine resolution region for extra timing points (to reject accidental tracks), corresponding to ±35 cm and ±80 cm in the front and back planes, respectively.

The vertical range covered by the front (back) detectors is from $y = \pm4.5$ cm to $y = \pm30$ cm (±5.5 to ±38.5 cm).

5.2 Narrow Detectors in High Resolution area

The front plane will mainly use the existing 84 2H8Y fingers to measure x, turned sideways so 2.54 cm deep, 1.27 wide, and 25.5 cm tall. They will be spaced with 2/3 overlap, in two adjoining sub-planes, with a center-to-center spacing of 1.692 cm on each sub-plane. These fingers cover ±17.7 cm in x. To make up the remaining ±8 cm, we plan to use 32 of the 64 2H3X fingers, which are 1.27 cm deep, 1.27 cm wide, and 20.5 cm long. To bring them up

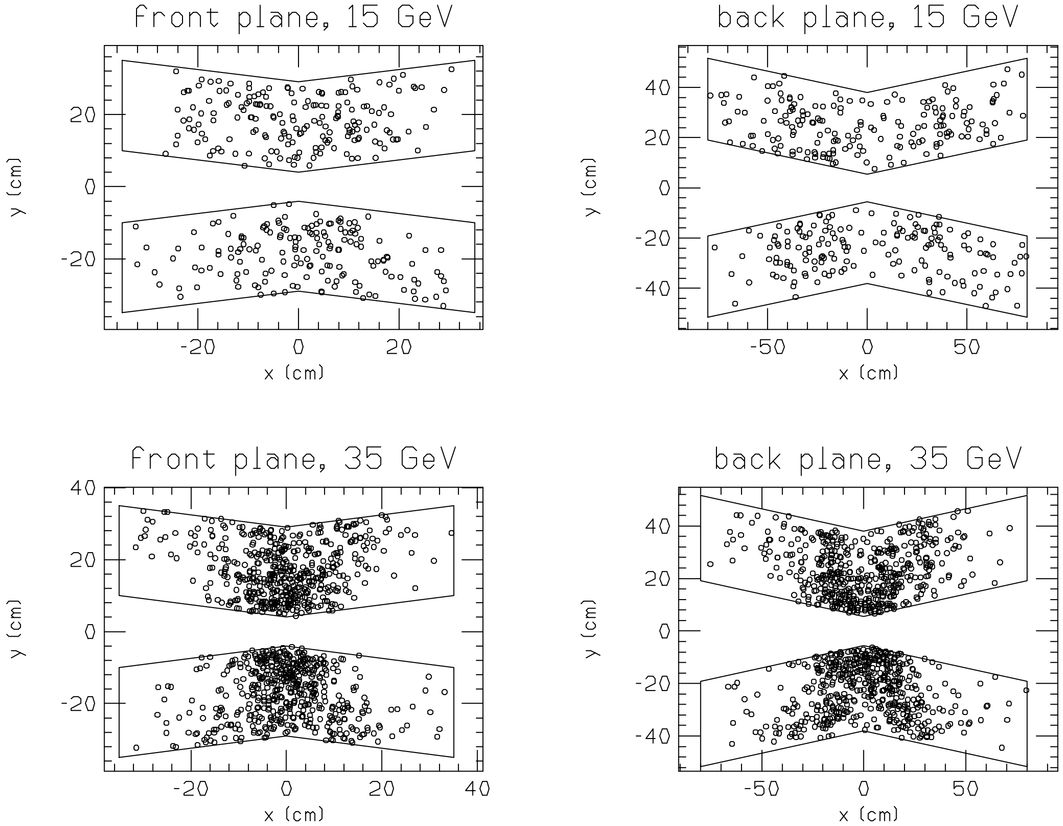

Figure 2: The overall dimensions of the front and back hodoscope plans are indicated by the "bow tie" shapes. The circles inside show the distribution of hits from muons coming from J/ψ decays at 15 GeV (top panels) and 35 GeV (bottom panels).

to 25.5 cm long, they must be lengthened by 5 cm using 11 of the pieces cut off the 2H7X fingers, which will be cut from 49.5 to 33 cm (see below).

For the back plane, to measure x, we will use the following 1.27 cm wide fingers with 2/3 overlap: the 90 2H7X fingers (shortened from 49 cm to 33 cm), the 72 2H4Y fingers, lengthened from 18 cm to 33 cm using the pieces cut from the 2H7X fingers, and the 32 (of 64) remaining 2h3X fingers (lengthened from 20.5 to 33 cm with new pieces). These combined give a coverage of ± 41 cm in x. To cover the remaining ± 19 cm, we will use the 88 2H1U/V fingers. These were originally 43 cm long, but presently 60 have been shortened to 1 cm. We will re-fasten the original fingers, shortened from 43 to 33 cm, once their use in E158 is completed. Because 11 of the pieces are no longer available, we will need 11 new 33 cm long pieces.

For y measurements, we plan to use the 49 10H3 fingers (76 cm long) in the back plane, with a spacing of 2.69 cm, to cover the ± 33 cm region. There will be small gaps between the fingers (0.13 cm) which will be covered by new fingers. For the front plane, we plan to use the 61 2H3Y and 5H3Y fingers, cut from 43 to 33 cm, with 1.6 cm spacing to cover ± 25 cm in y. All of these y fingers will have an angle of 0.17 rad with respect to the horizontal

Table 3: Dimensions and deployment of the existing E155 hodoscope fingers for E160. The variable length 45 degree fingers are not shown.

Use in	Num	Length (cm)	width (cm)	depth (cm)	tube diam.	old name
Back (x)	60	$1.0 \rightarrow 33$	1.5	0.6	3/4"	2H1U/V
Back (x)	28	$43.1 \rightarrow 33$	1.5	0.6	3/4"	2H1U/V
F/B. (x)	64	$20.5 \rightarrow 25/33$	1.27	1.27	1/2"	2H3X
Back (x)	72	$18.0 \rightarrow 33$	1.27	1.27	1/2"	2H4Y
Back (x)	90	$49.5 \rightarrow 33$	1.27	1.27	1/2"	2H7X
Front (x)	84	$25.5 \rightarrow 25$	1.27	2.54	1/2"	2H8Y
Front (y)	36	$43.0 \rightarrow 35$	3.00	0.64	1/2"	5H3Y
Front (y)	25	$43.0 \rightarrow 35$	3.00	0.63	1/2"	2H5Y
Back (y)	49	76.2	2.54	0.95	3/4"	10H4/5
?	23	69.0	3.00	0.64	1/2"	5H2X
?	34	58.9	2.00	0.63	1/2"	2H6X

axis to avoid the unwanted BH muon region. The ends of the fingers will slightly overlap near $x = 0$.

In total, about 45 new pieces will need to be purchased to obtain the desired lengths for the E155 hodoscopes. The remaining fingers will be lengthened using pieces cut off of other fingers. A total of 508 fingers from E155 will be used. Table 3 summarizes the plans and dimensions of the E155 fingers. Note that there are 57 fingers not presently assigned a use.

High voltage for the E155 fingers will be supplied by the new CAEN supplies, going to 2 way splitters. This will require about 256 channels of HV.

5.3 New hodoscope fingers

We plan to purchase 500 new hodoscope fingers. These fingers will all be 2.5 cm wide, and of various lengths. They will be spaced with 2/3 overlap, so that the effective spacing is 1.66 cm. A total of 84 (60) fingers will used to measure x (y) in the front plane, and 192 (80) fingers will be used in the back plane. The remaining 84 fingers will be used to measure y in the "muon" plane. The finger parameters are listed in Table 4.

The fingers will be read out by 1-inch Hamamatsu PMT's, with built-in tube base and HV supply. The fingers will not be glued to the PMT's, so that fingers of different length can readily be attached for used in other experiments, such as E161.

Table 4: Dimensions and deployment of the new hodoscope fingers for E160. The width of all fingers is 2.5 cm, and the depth is 1 cm.

Use in	Num	Length (cm)
Front (x)	84	25 cm
Front (y)	60	35 cm
Back (x)	192	33 cm
Back (y)	80	80 cm
Muon (y)	85	100 cm

6 Optics and Acceptance

To study the optics and acceptance, sets of J/ψ and ψ' particles were generated at energies of 15, 25, and 35 GeV, in the ratio of 50 to 1 to match the expected ratio of cross sections times branching ratio. The t distribution of the J/ψ mesons was modeled as e^{2t}, with an angular decay distribution into two muons of $[1 + \cos^2(\theta_{cm})]$.

The acceptance for di-muons from J/ψ decay was optimized with the following constraints: the detectors should be out of the "sheet of flame" region of the thousands of low invariant mass Bethe-Heitler muons per spill (see below); the detectors should mainly detect muons that pass through the hadronic filter, rather than the copper coils of the dipole, or the yoke iron; and the front detector should be as small as possible to minimize sprinkle hit rates. This results in principally selecting muons that both bend horizontally towards the beam pipe, coming close to a focus point near the front detector. A selection of horizontal ray traces for 15 and 35 GeV J/ψ decays is shown in Fig. 3. The tracks are for muons pairs for which both muons hit both the front and rear detectors. The traces tend to cross near the front detector, and spread out again towards the back detector. In the vertical plane (not shown), the tracks are nearly straight, except for a small curvature introduced by the fringe field of D3 (effectively a pole face rotation), and the x-component of the field map for muons that pass through the yoke near the end of D3.

Fig. 4 shows the acceptance as a function of the kinematic variables p_t^2, $\cos(\theta_{cm})$, and ϕ_{cm} for the 15, 25, and 35 GeV J/ψ momenta. The p_t^2 acceptance is quite uniform, which is a desirable feature for separating coherent, quasi-elastic, and inelastic production using the different t distributions for these processes (see E160 proposal). The $\cos(\theta_{cm})$ distributions are peaked near zero, which is optimal for minimizing backgrounds from Bethe-Heitler muon pairs (see [1]. The ϕ distribution is peaked near 180 degrees, corresponding to J/ψ decays that preferentially lie in the horizontal plane of the spectrometer. The total acceptance (defined as fraction of generated particles that pass through all detectors) is listed in Table 5. The acceptance is approximately the same for J/ψ and ψ' , and decreases rapidly as the J/ψ momentum decreases (because of the larger opening angle between the two muons), but is still at an acceptable level at 15 GeV.

Table 5: Resolutions and acceptance for the D3 spectrometer.

J/ψ momentum	15 GeV	25 GeV	35 GeV
Mass Resolution J/ψ (%)	4.4	4.2	4.0
Mass Resolution ψ' (%)	4.0	4.3	3.9
J/ψ Energy Resolution (%)	8.6	6.3	5.7
p_t Resolution (GeV)	0.16	0.12	0.12
J/ψ Acceptance	0.0058	0.0297	0.0559
ψ' Acceptance	0.002	0.028	0.043

7 Resolutions

The resolution in J/ψ invariant mass, energy, and transverse momentum are listed in Table 5 for incident photon energies of 15, 25, and 35 GeV. All values match those needed to adequately separate quasi-elastic J/ψ and ψ' production from coherent production (using the p_t distribution), from inelastic production (using both energy and p_t distributions), and high-mass Bethe-Heitler di-muon pairs (see extensive discussion in [1]). These resolutions were calculated using bosted/jpsi/d3spect.f, and approximately verified using the GEANT Monte Carlo. The simulation takes into account the detector granularity, multiple scattering, and energy loss fluctuations for muons passing through all materials, as well as the D3 magnetic field map. Tracking for obtain reconstructed muon kinematics was done in two methods: a look-up table using the full field map, generated with a large sample of muons of various momenta and angles; and a simplified analytic reconstruction based on a uniform field. The two methods are in reasonable agreement.

8 Rates

The J/ψ rates were modeled using a fit to world data for the total cross section, and a t dependence appropriate to quasi-elastic production (see above). A fit to the D3 spectrometer acceptance as a function of J/ψ momentum was used. The target parameters are given in [3]. The final input was the photon spectrum, for primary coherent peak energies of 15, 25, and 35 GeV (see [4]). The intensity was adjusted to allow the desired statistical error of 7% (after the large background subtractions, see [1]) on the ψ' A-dependence at 25 and 35 GeV, which then gives a higher rate of J/ψ events than in the proposal (which called for about 10,000 clean J/ψ events per target) by about a factor of three. The extra counts can be put to good advantage to reduce systematic errors on the separation of quasi-elastic events from other processes. The intensity at 15 GeV was adjusted to give about 3000 J/ψ events on each of two targets in 6 days, about a factor of two higher than in the proposal. The photon spectra (labeled Flux15, Flux25, and Flux35 for the coherent peaks at 15, 25, and 35 GeV respectively) are shown in Fig. 5. As will be seen below, these photon spectra intensities are fairly well matched to the maximum tolerable background rates in the

Table 6: Electron and photon beam parameters, J/ψ rates, goals, and number of ideal days needed for the E160 experiment, for each of the three settings. A repetition rate of 120 Hz is assumed.

Electron Energy (GeV)	45.0	45.0	48.3
Electron Current (10^{10}/spill)	5.0	5.0	5.0
Peak Photon Energy (GeV)	14.8	26.5	35.2
Collimator Radius (mm)	1.0	1.5	1.5
Diamond thickness (r.l.)	0.0040	0.0040	0.0040
Diamond angle (μrad)	305	888	1590
$k > 2.5$ GeV Photons/spill	1.1×10^9	5.8×10^8	3.8×10^8
Linear Polarization at Peak	0.91	0.68	0.47
J/ψ/day total	16757.	26382.	27876.
J/ψ/day in Peak	1003.	8299.	9900.
J/ψ goal per target	3000.	30000.	30000.
days (at 100% efficiency)	6.0	14.5	12.1

detectors,

The beam parameters, linear polarization at the top of the primary coherent peak, the total quasi-elastic J/ψ rate per day from a 1 gm/cm^2 target, the corresponding rate in the primary coherent peak, and the number of 100% efficiency days needed at each energy are listed in Table 6. It can be seen that even though the D3 spectrometer has a much lower acceptance than the LASS spectrometer design, the much higher beam flux possible with this design means that the experiment can be done in 30 ideal days, and still reach the proposal goals for the ψ' accuracy, and exceed the goals for the J/ψ . Note that the experimental goal only considers the J/ψ particles in the region of the primary coherent photon peak region: including the endpoint region will essentially give a high statistics point near 42 GeV for free, not mentioned in the original proposal. This can be seen in Fig. 5, which shows the predicted rate of quasi-elastic J/ψ particles as a function of their momentum (approximately the same as the photon beam energy).

9 Detector Backgrounds

Because the ψ' cross section, branching ratio, and acceptance result in very low rates, we would like to run at high a photon flux as possible. The limiting factor appears to be background rates in the detector. Given a spill length of about 250 nsec, we probably cannot reliably track more than about 20 particles per spill, and would like to limit the random sprinkle hit rate per hodoscope finger to a few per beam spill to keep the dead time at a reasonable level, and to avoid large numbers of accidental coincidences [5]. We have therefore simulated the rates from the principal sources of particles interacting with the filter and collimator in the spectrometer, using the GEANT Monte Carlo. This study was

Table 7: Rates of charged particles/spill/finger for the physics processes indicated, for typical Front or Back hodoscope fingers, and photon beam profiles Flux15 and Flux25. The principal type of charged particle(s) is also indicated.

Process	Particles	Front/Flux15	Back/Flux15	Front/Flux25	Back/Flux25
Hadronic	e, π, p	1.0	0.5	1.0	0.5
Compton	e^-/e^+	0.3	0.2	0.2	0.1
Primakov	e^-/e^+	0.3	0.2	0.2	0.1
e^-/e^+ Pairs	e^-/e^+	< 0.2	< 0.1	< 0.2	< 0.1
Total		1.6	0.9	1.4	0.7

used to optimize the choice of filter material (alumina in D3) and the tungsten collimator design. The next subsection present the results with the final design: for details on other configurations, see bosted/E160/geant/notes.m1.

Table 7 summarizes the number of charged particle hits/finger/spill calculated with GEANT for the physics processes described below. The rates are for the x-measuring, 2.5 cm wide fingers. The rates for the narrow fingers will be about half as much, and the rates for the y-measuring fingers will be somewhat larger. Rates are given for both the front and back hodoscope planes, and for two photon flux distribution profiles, corresponding to the 15 GeV (Flux15) and 25 GeV coherent peaks (Flux25). The rates for the 35 GeV setting are lower, and are not listed. The hadron and Compton rates scale with target thickness in gm/cm^2, and are given for the thickest target (Be), while the pair and Primakov rates scale with r.l., and are given for the target with the most r.l. (lead). Therefore the total rates are somewhat overestimated. On the other hand, the simulations probably cannot be trusted to better than a factor of two in any case, because the GEANT Monte Carlo does not have a complete treatment of all possible particle interactions, and is known to be inadequate for accurate evaluation of neutron-related backgrounds.

The hits are fairly evenly distributed over the detectors for all of the processes studied.

9.1 Hadronic Events

The largest number of hits in the hodoscopes come from hadronic interactions, in which a photon is totally absorbed on a proton or neutron in the target, and a hadronic final state is produced that usually includes several pions, at least one baryon, and often kaons and photons from π^0 decays. The event generator PYTHIA [6] was used to generate lists of all particles above 4 GeV momentum produced by the photon beam spectrum for one beam spill. An earlier study showed that particles below 4 GeV essentially never penetrate through the absorber in D3, and so were dropped to save computer time. About 110,000 particles were generated for Flux15, and about 93,000 particles for Flux25. The particle list was then fed into the GEANT simulation, and a record was kept of all particles that passed through the front or rear hodoscope planes. The charged particles were found to

Table 8: Number of hits in one beam spill and average energy (GeV) in the front and back planes for the hadronic background generated with Flux15. The last column shows the number of events that hit both the front and back plane at the same time. The total number of parent particles that made charged particle hits in this spill was 93.

	Front		Back		
particle	hits	$< E >$	hits	$< E >$	tracks
electrons	17	0.223	12	0.311	3
muons	3	1.436	34	1.855	2
pions	8	2.618	5	1.959	3
protons	60	0.014	8	0.023	1
neutrons	310	0.022	118	0.036	33
photons	194	0.010	152	0.013	37

be mostly positrons and protons, with also a few pions and muons per spill (see Table 8 for the total hits in the front and back planes by particle type for Flux15). It was noticed that the parents of these particles tend to be high momentum ($>$ 30 GeV) pions or K^0 (long), originating from high energy photons in the beam. Quite often, the parent particles produces a shower of particles, localized to the same detector region, which in the tracking code would look quite different than random sprinkle hits. These showers could be identified by a set of hits in many disjoint fingers, all at the same moment in time. Every hit has been saved to a file, and a future project is to do a complete tracking simulation including all the time correlations within a spill. However, experience from past experiments indicates that an average rate of about 1 hit/finger per spill is tolerable, and this is approximately what is observed.

The simulation also records the number of events for which a coincidence is observed between the front and back planes (see Table 8). Without taking into account geometrical cuts on the track directions (i.e. the track should point back to the target in the y direction), a total of 8 (8) tracks were found for one beam spill for Flux15 (Flux25), about equally divided between electrons, muons, pions, and protons. Very few of these tracks would pass the geometrical and momentum cuts. Although a complete simulation has not been performed of the tracking yet, experience from E155 indicates that a rate of 10 tracks/spill (before cuts) is quite tolerable, especially given that the ultimate tracking goal is to search for two separate muons tracks in time coincidence within a several hundred nanosecond long beam spill.

9.2 Compton Background

The cross section formula for atomic Compton scattering was used together with the Flux15 and Flux25 photon beam profiles to generate sets of scattered photons from the Be target. About 5000 (3000) photons above 1 GeV are produced each beam spill, with characteristic transverse momenta of about 0.1 GeV. These were passed into the GEANT Monte Carlo, from which it was found that a tungsten collimator is crucial to prevent the detectors from being illuminated by electromagnetic showers from small angle, high energy photons. Using lead instead of tungsten gave about a factor of three higher rates, at which point the Compton events dominate the singles rates in the back detectors, so it is strongly prefered to use Tungsten. Essentially all the hodoscope hits are electrons or positrons coming from secondary photons interacting in the hodoscopes. The typical charged particle energy is 10 MeV. Quite often, more than one hit is produced from a single primary photon, making a characteristic "spray" in the hodoscopes that should be distinct from real muon tracks, but introduces significant dead time into the TDC's for the local region of the hodoscope array.

9.3 Coherent π^0 production

The Primakov reaction ($\gamma A \rightarrow \pi^0 A$) cross section is proportional to Z^2, and is not negligible for the lead target [7]. The rates of photon pairs from the decay of these π^0's was calculated for the 0.12 r.l. lead target and the standard photon flux distributions, with a reasonable approximation for the π^0 momentum vector. The simulation predicts about 9000 (5000) decay photons above 1 GeV for the two flux distributions, with typical energies of 5 to 30 GeV, and typical transverse momenta of 0.06 GeV. These rays are quite similar, by chance, to the atomic Compton rays. The sprinkle hit rate from the Primakov process is on the order of 0.1 to 0.3 hits/finger/spill, tolerable but not insignificant range.

9.4 Electron/Positron Pair Production

By far the most common process for a photon interacting with a nucleus is pair production of an electron and positron, with characteristic angles of m_e/k. Since the rate per radiation length is about 0.8, over 10^8 pairs are generated per spill from the 0.12 r.l. targets. It would take too long (about 50 days) to simulate a full beam spill with this many pairs, so instead a sample corresponding to 0.01 beam spills was generated. The electron/positron pairs were all generated at zero degrees, with a uniform distribution in relative energy, which is a reasonable approximation for the vast majority of pairs. No charged particles were observed in the hodoscopes, but two photons passed through the front plane for the Flux15 file (but none through the back plane). Scaling by a factor of 100, then a few percent conversion probability per hodoscope plane, it appears that backgrounds from Bethe-Heitler electron/positrons is small compared to the other backgrounds studied. However, the tungsten collimator is crucial: a study with the collimator removed showed much higher rates.

9.5 Di-Muon Pair Production

Although Bethe-Heitler di-muons are rate compared to electron/positron pairs (by approximately a factor of $(m_e/m_\mu)^2$), the rate from the 0.12 r.l. targets is not negligible, corresponding to several thousand per beam spill. Most of the di-muons have an invariant mass close to the threshold of $2m_\mu$, and a characteristic angle of m_μ/k. These small angles result in a “sheet of flame” of muons emerging from the spectrometer along the horizontal axis, spread vertically by multiple scattering and the spread in production angles. Using a carefully tested Monte Carlo computer code (bosted/jpsi/bhs.f) adopted from [8], muon pairs were generated for the lead target for the coherent, quasi-elastic, and inelastic processes. A total of 2000 (1300) muons were generated for Flux15 (Flux25). These were then passed through the spectrometer ray-trace program (bosted/jpsi/d3spect.f), resulting in typical hit patterns as shown in Fig. 6 for the front and back planes. It can be seen that the “bow-tie” detector arrangement is crucial to minimize the number of muons per beam spill. We find zero (13) total hits in the front (back) plane (summed over all fingers) for Flux15, and zero (4) hits in the front (back) plane, for Flux25. This rate should be quite tolerable, as it is well below the rate from hadronic events. It turns out that all the hits are from low momentum muons with just enough energy to pass through the alumina and magnet iron.

9.6 Further Work Needed

The PYTHIA generator only generates hadronic events from a nucleon (proton or neutron), and has no provision for nuclear reactions. Coherent processes other than the Primakov reaction (considered above) may be important.

Another reaction that has not been considered is inelastic forward Compton scattering from nuclei. The elastic rate from a nucleon is very small at high energies (s^{-6} scaling), and a preliminary estimate of the inelastic rate indicates that it will be small compared to atomic Compton scattering.

A future project will be to write a realistic tracking code, input all the hits generated from the various background processes, and make sure that the overall efficiency and purity for finding the J/ψ decay events of interest are acceptable for the experiment, as we expect from previous experience. This study may lead to a better optimized detector arrangement.

References

[1] P. Bosted, “E160 Physics Requirements”, RPC-TN7, http://www.slac.stanford.edu/exp/e161/technical_notes/requirements_e160.ps.

[2] P. Bosted, “Spectrometer Design Options for E160”, RPC-TN13, http://www.slac.stanford.edu/exp/e161/technical_notes/spectdes_e160.ps.

[3] P. Bosted and K. Griffioen, “Targets Requirements for E160”, RPC-TN12, http://www.slac.stanford.edu/exp/e161/technical_notes/target_e160.ps.

[4] P. Bosted, “Photon Beam Requirements for E160 and E161”, RPC-TN11, http://www.slac.stanford.edu/exp/e161/technical_notes/photonbeam_e160.ps.

[5] S. Rock, “Tracking Background”, RPC-TN2, http://www.slac.stanford.edu/exp/e161/technical_notes/tracking_background.ps.

[6] T. Sjostrand, Computer Physics Commun. 82, 74 (1994).

[7] K. Griffioen, "Background Estimates from Primakov Pi0 Production", http://www.slac.stanford.edu/exp/e161/technical_notes/Polarimetry_E160.pdf.

[8] R. Yoshida, Nucl. Instrum. Meth. A302 (1991) 63.

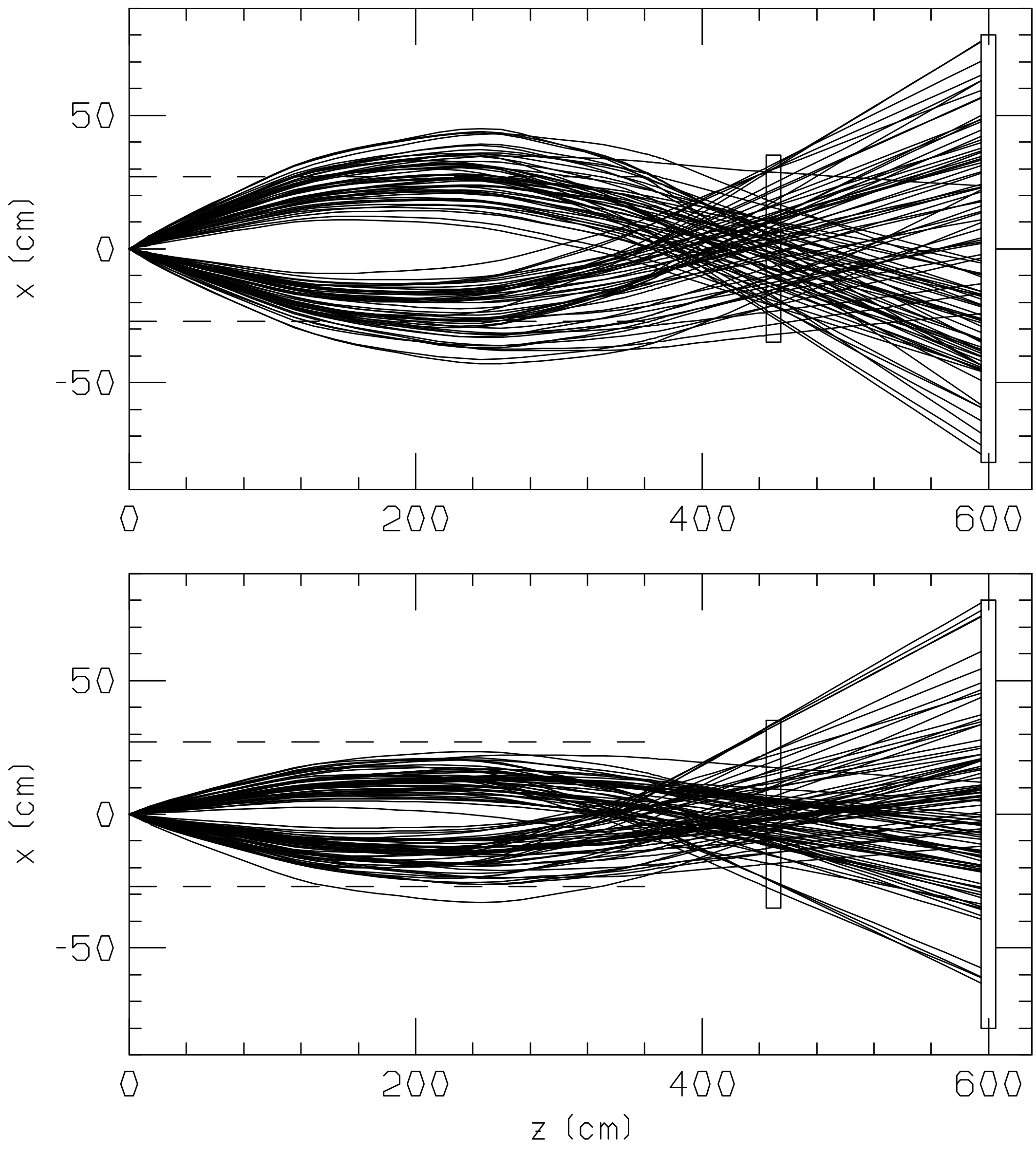

Figure 3: Ray trace of muon pairs from 15 GeV (top panel) and 35 GeV (bottom panel) J/ψ decays that pass through both front and back detectors (shown as boxes). The dashed lines show the D3 coils: many of the 15 GeV decay muons pass through these coils, while almost none of the 35 GeV muons do.

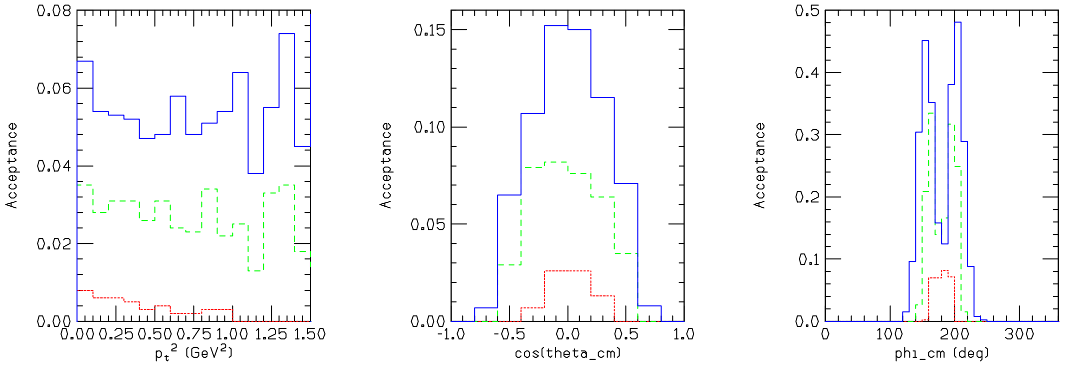

Figure 4: Acceptance for J/ψ particles as a function of transverse momentum squared p_t^2, $\cos(\theta_{cm})$ of the decay into two muons, and ϕ_{cm} of the decay, where 0 and 180 degrees are on the horizontal plane. The dotted, dashed, and solid curves correspond to 15, 25, and 35 GeV particles, respectively (colors red, green, and blue).

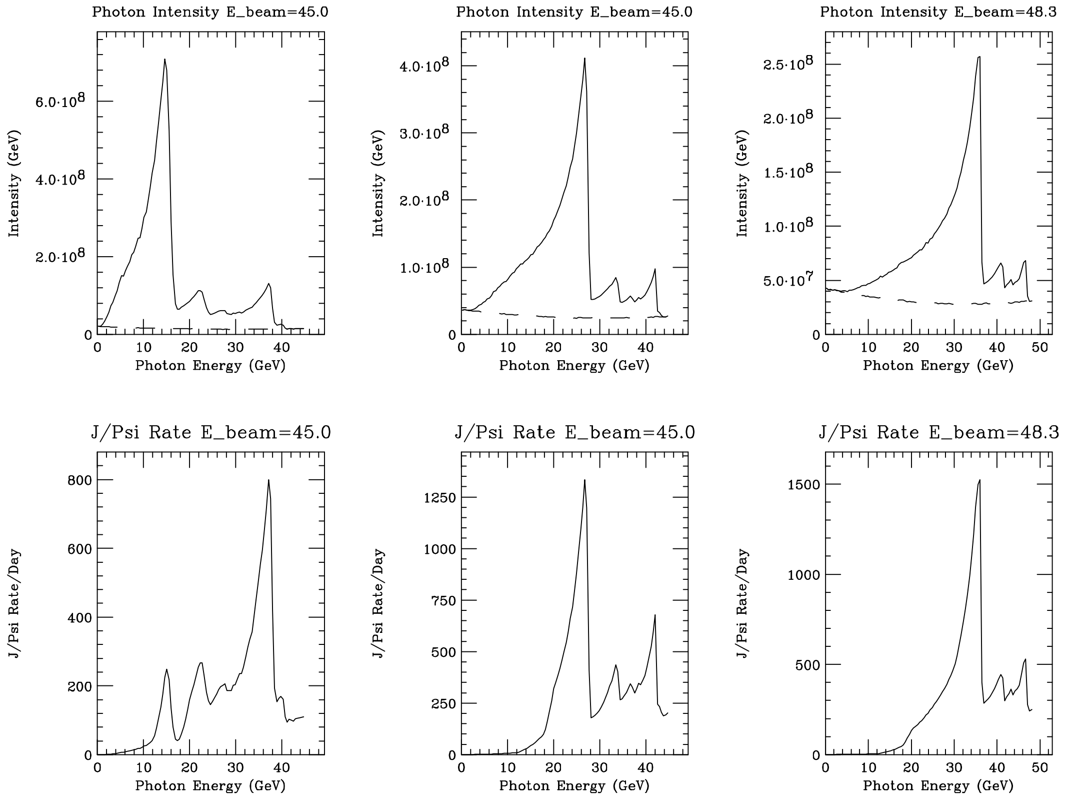

Figure 5: The top panels show the photon intensity spectra (flux times energy) as a function of photon energy for the primary coherent peak settings of 15, 25, and 35 GeV (from left to right), for one beam spill. The lower panels show the corresponding J/ψ rate per day for a 1 gm/cm^2 target.

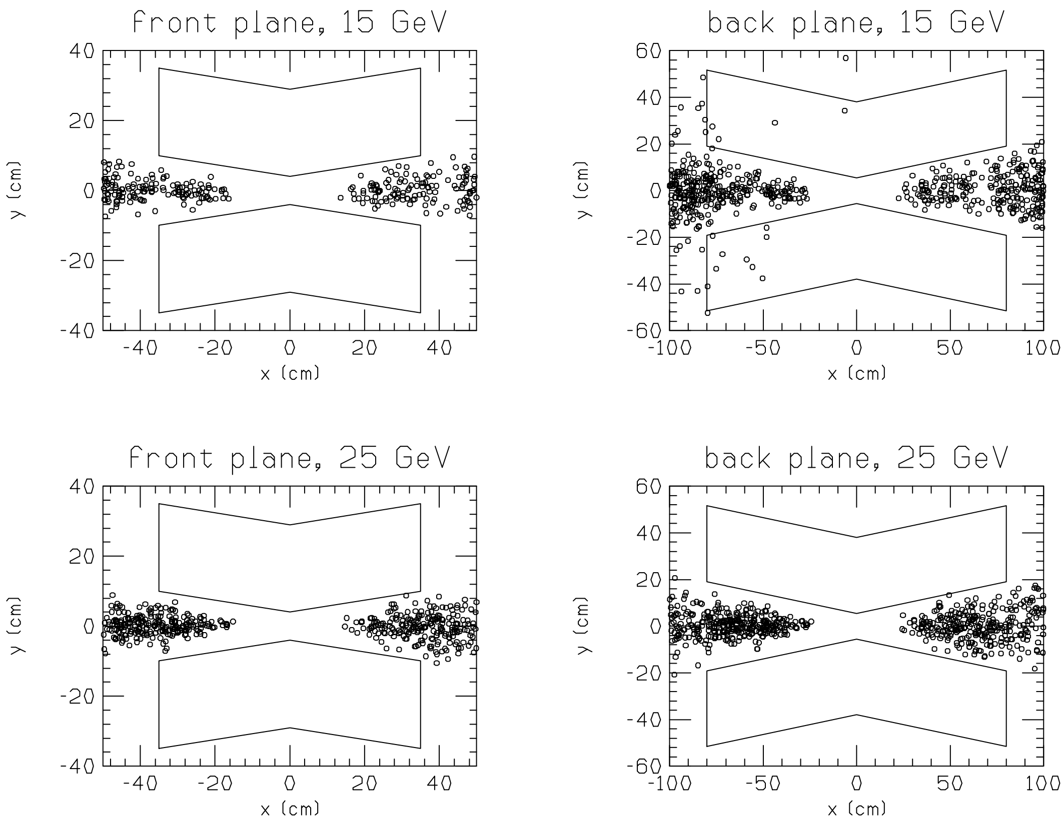

Figure 6: The overall dimensions of the front and back hodoscope plans are indicated by the “bow tie” shapes. The circles inside show the distribution of hits from muons from Bethe-Heitler pair production.